Three-dimensional left ventricular segmentation from magnetic resonance imaging for patient-specific modelling purposes

Enrico G. Caiani[1]*, Andrea Colombo[1], Mauro Pepi[2], Concetta Piazzese[1,3], Francesco Maffessanti[4], Roberto M. Lang[4], and Maria Chiara Carminati[1,2]

[1]Dipartimento di Elettronica, Informazione e Bioingegneria, Politecnico di Milano, Piazza L. da Vinci, 32, 20133 Milan, Italy; [2]IRCCS Centro Cardiologico Monzino, 20138 Milan, Italy; [3]Center for Computational Medicine in Cardiology, Universitá della Svizzera Italiana, 6900 Lugano, Switzerland; and [4]Noninvasive imaging Laboratories, University of Chicago Medical Center, 60637 Chicago, USA

Received 8 August 2014; accepted after revision 8 August 2014

Introduction

Cardiovascular disease is still the leading cause of death in most industrialized countries. In the last decade, thanks to advancements in imaging technology and knowledge of physiological mechanisms, and to improvements in computational power, physiological computational models tailored to individual patient characteristics proved to be a valuable and versatile technology to improve personalized medical care in many disciplines,[1] and especially in cardiology.[2]

Diagnostic imaging plays a central role in patient-specific modelling, combining anatomical and physiological measurements to evaluate cardiovascular structure and function. Among them, cardiac magnetic resonance (CMR) represents the preferred imaging choice for the heart models. Advantages of cardiac CMR include its non-invasive nature, well-tolerated procedures, ability to modulate contrast in response to several mechanisms, and ability to provide high-quality functional and anatomical information in any plane and any direction. In particular, CMR is considered to be the reference

* Corresponding author. Tel: +39 02 2399 3390; fax: +39 02 2399 3360. *E-mail address*: enrico.caiani@polimi.it

What's new?

- Generation of a statistical shape model of the left ventricle (LV) using endocardial surfaces extracted from real-time three-dimensional (3D) transthoracic echocardiography, to be used for 3D segmentation by means of active shape modelling (ASM) algorithm.
- Intermodality application of the ASM to nearly automatically segment the LV endocardium on a stack of short-axis cardiac magnetic resonance images.
- Possibility to utilize the obtained 3D endocardial mesh in the creation of realistic patient-specific finite element models, in which LV apex and base are realistically defined.

method for measurement of ventricular volumes and systolic function.[3] However, unless specific non-conventional three-dimensional (3D) sequences are utilized, cardiac CMR is a 2D imaging modality, limited by slice thickness, in- and out-of-plane motion of the cardiac structures, and potential misalignment among slices, due to both electrocardiographic (ECG) triggering and different apnoea phases in which image acquisition is performed.

These intrinsic constraints are reflected in the accuracy of the anatomical information that can be extracted and used to define the geometry of the left ventricle (LV) for modelling purposes. While LV endocardial manual tracing in each short-axis (SAX) image of the acquired stack represents the CMR 'gold standard' analysis modality to define LV geometry and compute LV volumes, it requires extensive time to be performed, thus being limited to selected patients. Moreover, geometrical 3D models obtained as spatial interpolation of the stack of 2D LV contours, are prone to distorsion if slice misalignment is present, and characterized by low resolution in-between slices, resulting in poor representation of the LV base and apex.

To facilitate LV endocardial contour extraction process, a variety of segmentation techniques have been proposed over the last few decades.[4] In particular, methods based on model-fitting segmentation, such as active shape modelling (ASM)[5–7] attempting to match a predefined geometric shape to the locations of the extracted image features, appear to be extremely promising. They are usually based on a two-step procedure: first, generating the shape model (including information about the shape and its variations) from a training set, and then performing the fitting of the model to a new image, thus solving an optimization problem of finding the best model parameters for a given patient image, where instances of the model can only deform in ways found in the training set.

Previous work has been done using ASM to segment the LV, and also other cardiac chambers from CMR images.[8–10] However, a potential limitation in previous applications arises from the fact that the generation of the 3D shape model is built from manual tracing of 2D SAX CMR slices in the training sets, and subsequent interpolation to derive the 3D endocardial surfaces. In this way, detailed anatomical information along the LV long-axis cannot be included in the ASM.

We hypothesized that the utilization of an intrinsically 3D training set, obtained by segmenting the LV endocardium from real-time 3D echocardiographic (3DE) images, could overcome this limitation, and be utilized to obtain the shape model for CMR segmentation. Accordingly, our aim was: (i) to define a strategy to automatically generate the shape model from a large set of LV 3D endocardial surfaces; (ii) to adapt its ASM evolution, with minimal user interaction, to the information included in the stack of CMR SAX images; (iii) to compare the results of this nearly automated segmentation, in terms of endocardial surface and therefrom derived LV volumes and ejection fraction (EF), using as 'gold standard' the conventional LV endocardial manual tracing of CMR SAX images.

Methods

First, the description of the ASM generation from a training set of 3DE images is given. Then, its application to CMR images in the group of analysed patients is described.

Shape model generation

Datasets of 205 subjects (122 normals, 19 with dilated cardiomyopathy, 13 with aortic insufficiency, 11 with aortic stenosis, 28 with mitral regurgitation, and 12 with mitral stenosis) who underwent real-time 3D transthoracic imaging examination at the University of Chicago, IL, USA or at Centro Cardiologico Monzino, Italy, were retrospectively selected. All 3DE acquisitions were performed using a iE33 (Philips) ultrasound system with X3-1 probe, using wide-angled modality in which wedge-shaped sub-volumes ($93^\circ \times 21^\circ$) were obtained over four to seven consecutive cardiac cycles during a breath-hold with ECG gating. Three-dimensional echocardiographic datasets were analysed for LV endocardial quantification by using semi-automated segmentation (4D LV analysis, Tomtec), from which detected surfaces along the cardiac cycle were exported as coordinates of 642 mesh nodes together with their connectivity matrix. In *Figure 1A*, an example of the exported mesh is shown, together with the position of the nodes corresponding to the LV apex (AP), mitral (MV), and aortic (AO) valve centres selected by the user during the segmentation process.[11] A total of 3284 3D LV surfaces obtained from the 205 subjects in the different frames of the cardiac cycle, which derived volumes ranged from 22 to 410 mL, were thus available for model generation.

As a first step, a registration operation of rototraslation was applied to co-register all the 3284 meshes to their centre of mass, LV long-axis, and angle of the line connecting AO and MV centres (*Figure 1B*). Scaling, based on LV apex-to-base distance, was not performed on purpose, to consider anatomical variability in the statistical variability described by the model.[12]

Ones all meshes were aligned, the mean LV endocardial surface was computed as average of the *x*, *y*, *z* coordinate positions for each corresponding node, and principal component analysis (PCA) was performed to find the minimal number of components able to describe the variability of all the points cloud.[5,13] The result of PCA is a set of principal axes of variation, computed as linear combination of the original coordinate system, describing the variability of the original data in descending order. In this way, we found that a total of 1926 principal components (PC) was needed to describe the whole variability in the data, but the first 5 PC were already able to describe its 75% variability, while 79 PC described 99.7% variability (*Figure 1C*).

Population and gold standard

Data from 12 consecutive patients (2 with normal LV function, 7 with ischaemic dilated cardiomyopathy, and 3 with myocardial infarction) referred for cardiac evaluations were considered for testing the performance of the proposed algorithm. Cardiac magnetic resonance images (1.5 T) were acquired using the conventional cardiac imaging sequence (FIESTA) in both two- and four-chamber planes, as well as in stack

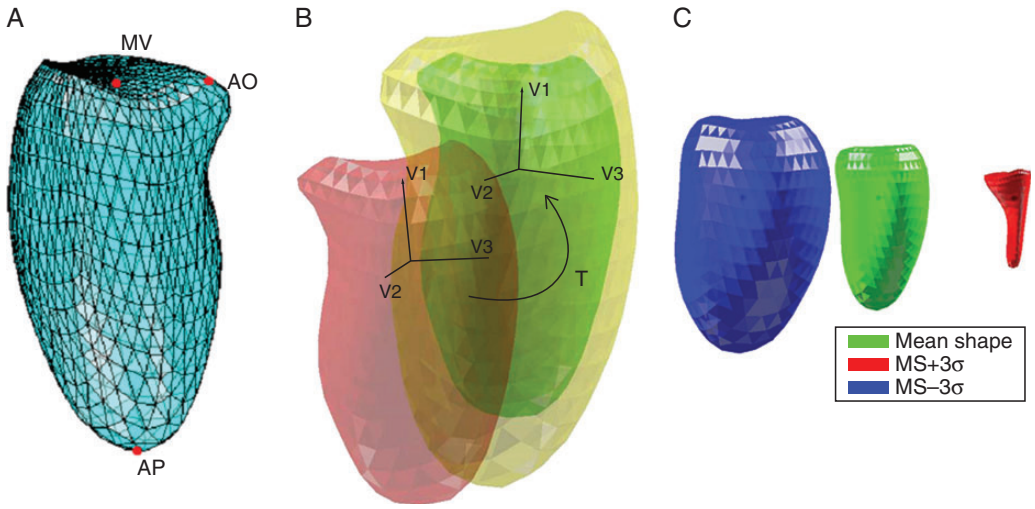

Figure 1 (*A*) Example of an endocardial LV surface obtained from the semi-automated segmentation of the 3DE dataset, with user-selected points corresponding to LV apex (AP), mitral (MV), and aortic (AO) valve centres. (*B*) Schematization of the rototraslation operation (T) applied to co-register all the 3284 LV endocardial surfaces to their centre of mass and LV long-axis. (*C*) Possible deformation of the mean shape model (in green) by changing the first PCA component only, so to represent the 99.7% variability included in the training dataset.

(from 6 to 13) of SAX planes to cover the entire LV (slice thickness 8 mm, no gap, no overlap). End-diastolic and end-systolic frames were visually selected for analysis as the frames showing maximal and minimal LV volume, respectively. Reference values for comparison were conventionally obtained by manually tracing the LV endocardial contour in each SAX plane, including papillary muscles in the LV cavity. Then, LV volumes were computed using a disc-area summation method (modified Simpson's rule). The end-diastolic (EDV) and end-systolic (ESV) volumes were used to compute the EF as 100*(EDV − ESV)/EDV. These parameters were used as 'gold standard' to test the measurement accuracy obtained with the proposed nearly automated 3D segmentation technique.

Pre-processing and cardiac magnetic resonance initialization

As the segmentation will be performed in 3D, using simultaneously all the information included in the stack of SAX planes, it is mandatory to correct for potential misalignment between long-axis and SAX planes, to avoid distortion in the final LV endocardial surface. To do so, a cross-correlation technique for in-plane correction was applied to each SAX plane.[14]

For each frame to be analysed, a six-point manual initialization procedure (two for mitral valve leaflet insertion and one for LV apex, in both apical four- and two-chamber views) is needed to: (i) scale the mean ASM model to the data to be analysed, based on LV apex-to-base distance along the long-axis; (ii) place the scaled model inside the stack of SAX CMR images; (iii) automatically define the SAX planes containing the LV (from base to apex), to be used to deform the model.

Model deformation

After these three steps, starting from this initial ASM model position in the stack of SAX CMR images, by considering the intersections of the 3D model with each SAX, the 3D mesh model is iteratively deformed to match the LV endocardial position in all SAX planes contemporaneously, until a stable condition is reached. This is achieved throughout the following steps:

(1) Determining the intersections of the model with the SAX image. The ASM model is a mesh constituted by triangular patches, so the patches intersecting the imaging plane can be determined, and two intersecting points for each patch identified (*Figure 2A*).
(2) Defining a research space. For each intersection, the pixel video intensity profile of the line connecting it with the centre of mass of all intersections[15] was extracted, and used to generate a 2D image L representing all the aligned profiles (*Figure 2B*).
(3) *K*-means clustering. The image L was processed using a *K*-means clustering, searching for five separate clusters to better represent blood in the LV cavity, myocardium, and external structures. Following this operation, a binarization was applied by considering as white the pixels classified as blood in the LV cavity, and as black all the others.[16] The interface pixels (*Figure 2B*) were then extracted, and used as the LV endocardial candidate position nodes in the iterative update process of the ASM mesh.
(4) To do so, a first rigid repositioning of the mesh in the actual SAX stack was performed by partial Procruste analysis.[17] Then, a displacement vector was computed for each node of the mesh, based on the position of the respective candidate points, and applied (*Figure 3A*).

These steps are applied recursively, with each new iteration starting from the position and configuration of the ASM mesh resulting from the previous iteration, until the computed model update does not produce a significant change in the mesh,[18] measured as the sum of all the nodes displacements greater than the CMR image spatial resolution.

Volume computation

On the final ASM endocardial mesh, LV volume was derived in two ways:

(1) direct volume computation, based on the sum of volumes of all the regular tetrahedral patches composing the 3D mesh (3D);
(2) to replicate 'gold standard' analysis, at each intersection of the ASM mesh with the original SAX planes, LV cavity area was computed, and LV volume derived using the disc-area summation method (2D).

Statistical analysis

Agreement between manual 'gold standard' measures and the result of semi-automated 3D segmentation by ASM was evaluated using Bland–Altman analysis. In addition, linear regression analysis was performed, and Pearson correlation coefficient was computed. The *t*-test was applied to verify the significance of the bias (paired *t*-test vs. null values).

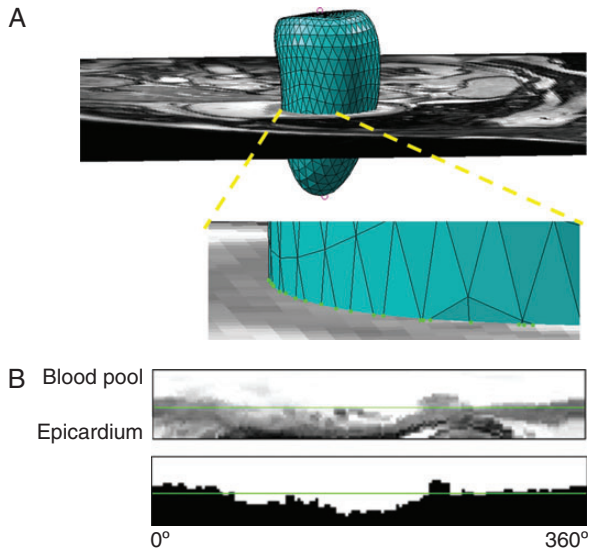

Figure 2 (*A*) Visualization of the intersections of the 3D model with one representative SAX plane, with zooming to evidence the two intersecting points (in green) for each triangular patch of the mesh. (*B*) Result of *K*-means clustering segmentation to obtain interface pixels that will guide model deformation in the next iteration.

Results

Algorithm implementation was performed in Matlab (MathWorks). Required time on a conventional laptop (IntelCore i7 @2.3 GHz, 6 GB RAM) to analyse a stack of 10 CMR SAX slices and obtain the LV 3D endocardial surface for one frame was $<$50 s, including 10 s for manual initialization. Conventional manual tracing for 'gold standard' determination took about 5 min per frame.

Gold standard analysis provided volume measurements in the range of 120–283 mL for EDV, 32–239 mL for ESV, and 16–73% for EF.

Figure 3B shows an example of the final ASM mesh superposed to an apical two-chamber long-axis view, from which it is possible to appreciate the correspondence of the detected surface to the LV endocardial position in the CMR image, as well as the anatomical description of the LV apex and base. This was confirmed in all cases, both with apical two- and four-chamber views superposed visualization.

Comparison of LV volumes (EDV and ESV) between the gold standard and the results of the segmentation, either as 3D mesh or as 2D method of discs resulted in slopes close to 1 and very high and statistically significant correlation coefficients (3D: $m = 0.99$, $r^2 = 0.97$; 2D: $m = 0.98$, $r^2 = 0.98$). Bland–Altman analysis showed in both cases no significant bias and narrow limits of agreement (*Figure 4*, top), corresponding to a per cent error of the measured volume of $\pm 22\%$ for 3D and $\pm 26\%$ for 2D compared with manual analysis. One outlier is visible in the graph, in which EDV, but not ESV, was underestimated compared with the 'gold standard', resulting in EF overestimation. While comparing EF, again slopes close to 1 and high and statistically significant correlation coefficients (3D: $m = 0.99$, $r^2 = 0.91$; 2D: $m = 1.01$, $r^2 = 0.90$) were found. In addition, no significant bias and narrow limits of agreement (*Figure 4*, bottom), corresponding to a per cent error of the measured EF of $\pm 27\%$ for 3D and $\pm 29\%$ for 2D compared with manual analysis were found by Bland–Altman analysis.

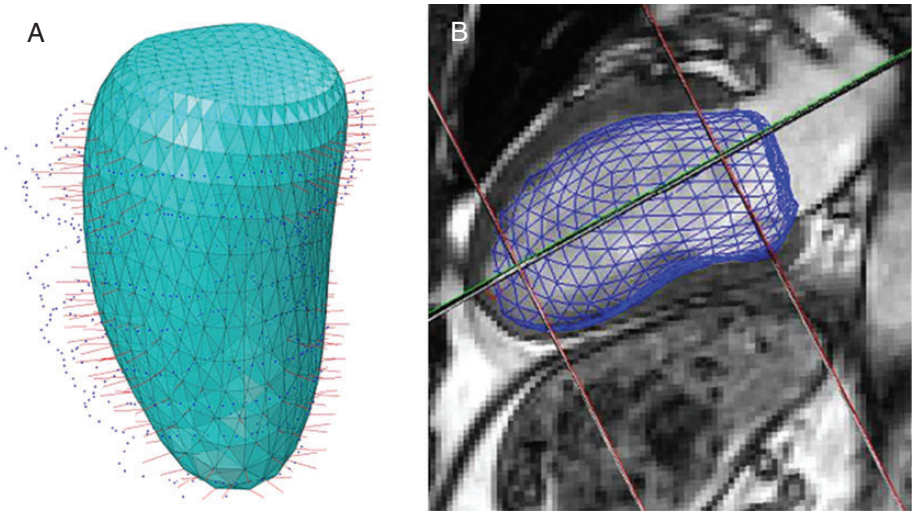

Figure 3 (*A*) Schematization of the model deformation in one step, where for each node of the ASM mesh a displacement vector is computed based on candidate points on the interface between blood in the LV cavity and tissue for each SAX plane intersection with the mesh. (*B*) Example of the resulting LV endocardial mesh, superposed to an apical two-chamber view to appreciate correspondence with the LV morphology.

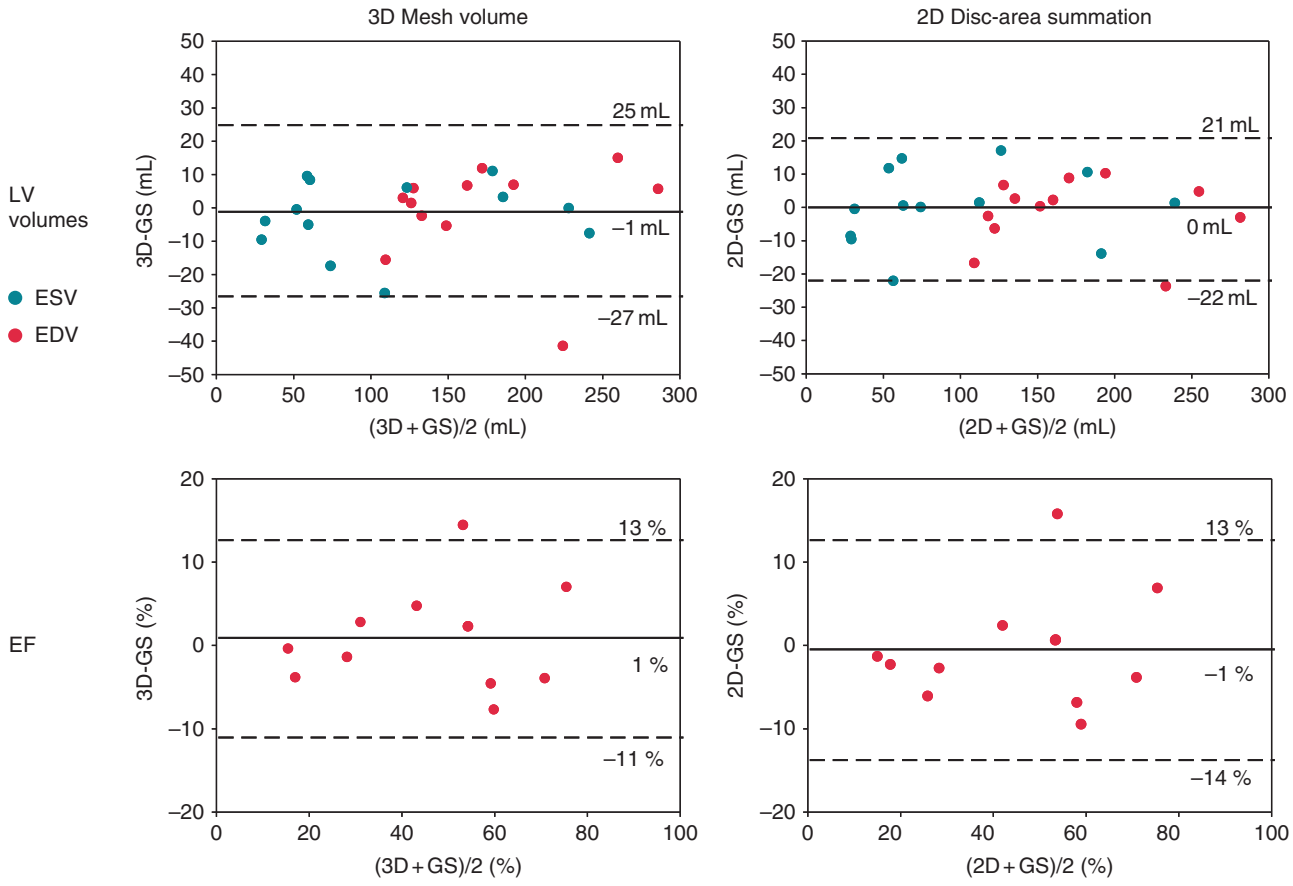

Figure 4 Bland–Altman analyses of the comparison between the 'gold standard' manually derived LV volumes and EF with respective values obtained from the segmented 3D endocardial meshes, both as direct volume computation and replicating the 2D disc-area summation method.

Discussion

Our main goal was to propose and validate a 3D CMR nearly automated LV endocardial segmentation procedure based on a novel intermodality ASM approach. To our knowledge, this is the first time that a statistical model is built based on 3D LV endocardial surfaces extracted from 3DE images, and then applied to segment CMR images, thus constituting a completely new intermodality approach.

Compared with ASM model creation using CMR or computed tomography images, 3DE has the advantage of being widely used and non-invasive, without contraindications in patients with implanted devices, thus providing the potential for further expanding the training dataset to different patients' groups. Moreover, using not interpolated and intrinsically 3D LV endocardial surfaces allows to obtain an ASM model consistent with LV anatomy, in particular in the representation of LV apex and base at the level of the mitral plane.

The proposed CMR segmentation procedure required minimal user interaction, with the selection of only six points on the long-axis views, and used this information to automatically position the model in the SAX stack and determining the slices range to be included in the segmentation process. On the contrary, previous ASM approaches required more extensive initialization[10] or manual localization of the initial model position[16] to work properly.

The ASM deformation process has shown to be computationally robust and fast, thanks to the pre-processing correction[14] for misalignments of the CMR images, taking into account contemporaneously the information derived from all the SAX planes including the LV, and properly evolving to represent the true apex and base, as confirmed by visualizing the resulting mesh with the superposed original CMR long-axis two- and four-chamber images.

The output of the endocardial segmentation is provided both as 2D LV contours on the original SAX images, to compute the LV volume as discs-summation method, and as a morphologically accurate 3D LV endocardial surface mesh, in a representation that can be easily integrated into a patient-specific finite element model for surgical planning[19] or cardiac mechanics study purposes.[20] The comparison with the conventional 'gold standard' analysis of LV volumes derived from CMR images showed the proposed method to be accurate, thus being potentially applicable in the clinical setting. In fact, independently of the strategy used to compute LV volumes from the 3D mesh (by direct computation or by 2D disc-area summation), no bias has been found compared with the 'gold standard', with slightly narrow limits of agreement for the direct computation ($\pm$22%) compared with the 2D assessment ($\pm$26%), probably due to the improved morphological definition at the LV apex and base.

Study limitations

We have presented a first pilot study to evaluate the feasibility and initial accuracy of the proposed intermodality ASM approach to segment cardiac CMR images. Its main limitation is that it has been tested on a limited number of patients undergoing CMR imaging. However, obtained results in the heterogeneous patient population analysed, not confined to a specific pathology, are promising.

An intrinsic limitation of the statistical shape methods is that the results of the segmentation are dependent from the original population used as database to generate the model. In fact, if a patient to be analysed has an LV shape that is not well represented in the database, the model is not able to fit it properly. As an example, in case of the analysis of a patient with extremely dilated LV ($>$410 mL), the segmentation would have resulted in a LV volume underestimation, as the model expansion is related to the extent of the morphological characteristics of the population used as training set, that did not include patients with LV $>$ 410 mL. In the same way, with the current training datasets, patients with right ventricular dilation due to pulmonary hypertension could not be analysed, as they were not included in the original database. The convexity in LV septum that characterizes patients with this pathology is indeed not represented in the 205 patients that generated the database, all with LV septal concavity. These limitations can be solved by adding to the database more LV endocardial surfaces extracted from specific patient groups, or with specific anatomical characteristics (i.e. extremely dilated).

Conclusions

In conclusion, we proposed a 3D CMR nearly automated LV endocardial segmentation procedure based on a novel intermodality statistical modelling approach. The utilization of 3D LV endocardial surfaces extracted from 3DE images as training datasets for model construction allows reproducing the correct LV morphology, thus resulting in a segmented 3D mesh including a realistic LV apex and base that could constitute the input for more realistic patient-specific finite element modelling.

Conflict of interest: none declared.

Funding

This work was supported by the Italian Space Agency (contract number 2013-032-R.0, recepient E.G.C.).

References

1. Neal ML, Kerckhoffs R. Current progress in patient-specific modeling. *Brief Bioinform* 2010;**11**:111–26.
2. Reumann M, Gurev V, Rice JJ. Computational modeling of cardiac disease: potential for personalized medicine. *Personalized Med* 2009;**6**:45–66.
3. Pattynama PMT, DeRoos A, Vanerwall EE, Vanvoorthuisen AE. Evaluation of cardiac function with magnetic resonance imaging. *Am Heart J* 1994;**128**:595–607.
4. Kang D, Woo J, Slomka PJ, Dey D, Germano G, Kuo C-CJ. Heart chambers and whole heart segmentation techniques: review. *J Electron Imaging* 2012;**21**:1–16.
5. Cootes TF, Cooper D, Taylor CJ, Graham J. A trainable method of parametric shape description. *Image Vis Comput* 1992;**10**:289–94.
6. Cootes TF, Hill A, Taylor CJ, Haslam J. The use of active shape models for locating structures in medical images. *Image Vis Comput* 1994;**12**:355–65.
7. Cootes TF, Taylor CJ, Cooper D, Graham J. Active shape models—their training and application. *Comput Vis Image Underst* 1995;**61**:38–59.
8. Kaus MR, Berg Jv, Weese J, Niessen W, Pekar V. Automated segmentation of the left ventricle in cardiac MRI. *Med Image Anal* 2004;**8**:245–54.
9. Lötjönen J, Kivistö S, Koikkalainen J, Smutek D, Lauerma K. Statistical shape model of atria, ventricles and epicardium from short-and long-axis MR images. *Med Image Anal* 2004;**8**:371–86.
10. Zhang H, Wahle A, Johnson RK, Scholz TD, Sonka M. 4-D cardiac MR image analysis: left and right ventricular morphology and function. *IEEE Trans Med Imaging* 2010;**29**: 350–64.
11. Verhey JF, Nathan NS. Feasibility of rapid and automated importation of 3D echocardiographic left ventricular geometry into a finite element analysis model. *Biomed Eng Online* 2004;**3**:32.
12. Heimann T, Meinzer H-P. Statistical shape models for 3D medical image segmentation: a review. *Med Image Anal* 2009;**13**:543–63.
13. Joliffe I. *Principal Component Analysis.* 2nd ed. New York: Springer-Verlag, 2002.
14. Carminati MC, Maffessanti F, Caiani EG. Nearly automated motion artifacts correction between multi breath-hold short-axis and long-axis cine CMR images. *Comput Biol Med* 2014;**46**:42–50.
15. Van Assen HC, Van der Geest R, Danilouchkine MG, Lamb H, Reiber JH, Lelieveldt BP. 3D active shape model matching for left ventricle segmentation in cardiac CT. *Proc SPIE—Int Soc Opt Eng* 2003;**5032 I**:384–93.
16. Van Assen HC, Danilouchkine MG, Dirksen MS, Reiber JH, Lelieveldt BP. A 3D Active shape model driven by fuzzy inference: application to cardiac CT and MR. *IEEE Trans Inf Technol Biomed* 2008;**12**:595–605.
17. Gower J. Generalized Procrustes analysis. *Psychometrika* 1975;**40**:33–51.
18. Cootes TF. Model-based methods in analysis of biomedical images. In Baldock R, Graham J (eds). *Image Processing and Analysis.* Oxford: Oxford University Press; 2000. p223–48.
19. Conti C, Votta E, Corsi C, De Marchi D, Tarroni G, Stevanella M *et al.* Left ventricular modelling: a quantitative functional assessment tool based on cardiac magnetic resonance imaging. *Interface Focus* 2011;**1**:384–95.
20. Trayanova NA, Boyle PM. Advances in modeling ventricular arrhythmias: from mechanisms to the clinic. *Wiley Interdiscip Rev Syst Biol Med* 2014;**6**:209–24.